

# Master Formulae Approach to Photon Fusion Reactions

C.-H. Lee<sup>a</sup>, H. Yamagishi<sup>b</sup> and I. Zahed<sup>a</sup>

*a) Department of Physics & Astronomy, SUNY at Stony Brook, Stony Brook, NY 11794, USA;*

*b) 4 Chome 11-16-502, Shimomeguro, Meguro, Tokyo, 153 Japan.*

We analyze the  $\gamma\gamma \rightarrow \pi\pi, KK, \eta\eta, \pi\eta$  reactions through  $\sqrt{s} = 2$  GeV, using the master formula approach to QCD with three flavors. In this approach, the constraints of broken chiral symmetry, unitarity and crossing symmetry are manifest in all channels. The pertinent vacuum correlators are analyzed at tree level using straightforward resonance saturation methods. A one-loop chiral power counting analysis at threshold is also carried out and compared to standard chiral perturbation theory. Our results are in overall agreement with the existing data in all channels. We predict the strange meson polarizabilities and a very small cross section for  $\gamma\gamma \rightarrow \eta\eta$ .

## I. INTRODUCTION

There is a wealth of empirical information regarding photon fusion reactions to two mesons both at threshold and above [1–10]. At low energy these reactions provide stringent constraints on our understanding of broken chiral symmetry and the way mesons and photons interact. At higher energy they reveal a variety of resonance structure that reflects on the importance of final state correlations and unitarity in strong interaction physics.

Some of these reactions have been analyzed using chiral perturbation theory [11], dispersion relations [12] and also effective models [13]. One-loop chiral perturbation theory [14] does well in the charged channels, but yields results that are at odd with the data in the chargeless sector, suggesting that important correlations are at work in the final states. Some of these shortcomings have been removed by a recent two-loop calculations [15] and the help of few parameters that are fixed by resonance saturation. The results are overall in agreement with an early dispersion analysis for  $\gamma\gamma \rightarrow \pi^0\pi^0$  [12]. Effective models using aspects of chiral symmetry and s-channel unitarisation have revealed the importance of final state interactions in most of these reactions [13,16].

Recently, a global and unified understanding of broken chiral symmetry was reached in the form of a master formula for the extended S-matrix [17]. A number of reaction processes involving two light quarks were worked out and shown to be interdependent beyond threshold. The approach embodies the essentials of broken chiral symmetry, unitarity and crossing symmetry to all orders in the external momenta. By power counting it agrees with standard chiral perturbation theory in the threshold region. It is flexible enough to be used in conjunction with dispersion analysis or resonance saturation techniques to allow for a simple understanding of resonance effects and final state interactions beyond threshold.

In this paper, we would like to give a global understanding of most of the fusion reaction processes using the master formula approach to broken chiral symmetry including the effects of strangeness. The present work confirms and extends the original analysis in the two flavour case [18]. In section II, we introduce our conventions for the fusion reaction processes, and discuss the essentials of the T-matrix amplitudes. In section III, we give the main result for the fusion reaction processes as expected from the master formula approach to QCD with three flavors. The importance of s-channel scalar correlations is immediately unravelled. In section IV, we analyze the general result in chiral power counting and compare to one-loop chiral perturbation theory with strangeness. In section V, we analyze the master formula result beyond threshold by using resonance saturation methods. In section VI, we discuss briefly the meson polarizabilities in our case. In section VII, a detailed numerical analysis of our results is made and compared to presently available data. We predict a small cross section for  $\gamma\gamma \rightarrow \eta\eta$ . Our conclusions are in section VIII. Some calculational details are given in three Appendices.

## II. GENERALITIES

### A. Conventions

We will consider generically the reactions  $\gamma^c(q_1)\gamma^d(q_2) \rightarrow \pi^a(k_1)\pi^b(k_2)$  with  $a, b = 1 \sim 8$  and  $c, d = 3, 8$  for the light mesonic octet. The photon polarizations are chosen in the gauge  $\epsilon_\mu(q_i)q_j^\mu = 0$  with  $i, j = 1, 2$ . Throughout, the Mandelstam variables are given by

$$\begin{aligned}s &= (q_1 + q_2)^2 = 2q_1 \cdot q_2 \\t &= (q_1 - k_1)^2 = k_1^2 - 2q_1 \cdot k_1\end{aligned}$$

$$u = (q_1 - k_2)^2 = k_2^2 - 2q_1 \cdot k_2 . \quad (1)$$

and both the photons and the mesons are on-shell,  $q_i^2 = 0$  and  $k_i^2 = m_a^2$ . Our convention for the electromagnetic current is standard

$$\mathbf{J}_\mu^{em} = \bar{q}\gamma_\mu \left( \frac{1}{2}\lambda_3 + \frac{1}{2\sqrt{3}}\lambda_8 \right) q = \mathbf{V}_\mu^3 + \frac{1}{\sqrt{3}}\mathbf{V}_\mu^8 , \quad (2)$$

so that the photon isospin indices are only 3 and 8. This will be assumed throughout.

### B. Helicity Amplitudes

The T-matrix for the fusion process  $\gamma(q_1)\gamma(q_2) \rightarrow \pi^a(k_1)\pi^b(k_2)$ , will be defined as [15]

$${}_{\text{out}}\langle \pi^a(k_1)\pi^b(k_2) | \gamma(q_1)\gamma(q_2) \rangle_{\text{in}} = i(2\pi)^4 \delta^4(P_f - P_i) \mathcal{T}^{ab} \quad (3)$$

with

$$\mathcal{T} = e^2 \epsilon_1^\mu \epsilon_2^\nu V_{\mu\nu}^{ab} . \quad (4)$$

The photons are transverse, that is  $\epsilon_i \cdot q_j = 0$ , hence

$$V_{\mu\nu} = A(s, t, u) T_{1\mu\nu} + B(s, t, u) T_{2\mu\nu} \quad (5)$$

with the invariant tensors

$$T_{1\mu\nu} = \frac{1}{2} s g_{\mu\nu} - q_{1\mu} q_{2\nu} \quad T_{2\mu\nu} = 2s(k_1 - k_2)_\mu (k_1 - k_2)_\nu - \nu^2 g_{\mu\nu} \quad (6)$$

and  $\nu = (t - u)$ . As a result, the T-matrix reads

$$\begin{aligned} \mathcal{T} &= e^2 \left( A(s, t, u) s/2 - \nu^2 B(s, t, u) \right) \epsilon_1 \cdot \epsilon_2 - e^2 8s B(s, t, u) \epsilon_1 \cdot k_1 \epsilon_2 \cdot k_2 \\ &= -2e^2 \epsilon_1 \cdot \epsilon_2 (\mathbf{1} - \mathcal{X}) - e^2 (\epsilon_1 \cdot k_1) (\epsilon_2 \cdot k_2) 8s (B_0 + \mathcal{Y}) \end{aligned} \quad (7)$$

with  $\mathbf{1}$  and  $B_0$  defined as

$$\begin{aligned} \mathbf{1} &= \begin{cases} 1 & \text{for } \pi^\pm, K^\pm \\ 0 & \text{for } \pi^0, K^0, \bar{K}^0, \eta \end{cases} \\ B_0 &= \mathbf{1} \frac{1}{2s} \left( \frac{1}{t - m_\pi^2} + \frac{1}{u - m_\pi^2} \right) . \end{aligned} \quad (8)$$

The corresponding helicity amplitudes are [15]

$$\begin{aligned} H_{++}^{ab} &= A^{ab} + 2((m_a + m_b)^2 - s) B^{ab} \\ H_{+-}^{ab} &= \frac{8(m_a^2 m_b^2 - tu)}{s} B^{ab} . \end{aligned} \quad (9)$$

### C. Polarizabilities

The differential cross section for unpolarized photons to two mesons in the center-of-mass system is

$$\begin{aligned} \frac{d\sigma^{\gamma\gamma \rightarrow \pi^a \pi^b}}{d\Omega} &= f_{ab} \frac{\alpha^2 s}{32} \beta^{ab}(s) (|H_{++}|^2 + |H_{+-}|^2) \\ &= f_{ab} \frac{\alpha^2}{4s} \beta^{ab}(s) \left( \left| \mathcal{B} + \frac{m_\pi}{2\alpha} s \alpha_\pi^{ab}(s) \right|^2 + \left| \mathcal{B}' + \frac{m_\pi}{2\alpha} s \alpha_\pi^{ab}(s) \right|^2 \right) , \end{aligned} \quad (10)$$

with the degeneracy factor

$$f_{ab} = \begin{cases} 1/2 & \text{for } \pi^0\pi^0, \eta\eta \\ 1 & \text{for other processes} \end{cases} . \quad (11)$$

The expressions for  $\mathcal{B}$ ,  $\mathcal{B}'$  and the polarizabilities  $\alpha_\pi^{ab}$  are

$$\begin{aligned} \mathcal{B} &= \mathbf{1} \left( -1 + \frac{2sm_\pi^2}{(t-m_\pi^2)(u-m_\pi^2)} \right) \\ \mathcal{B}' &= \mathbf{1} + 4(m_\pi^4 - tu)\mathcal{Y} \\ \frac{m_\pi}{2\alpha} s\alpha_\pi^\pm(s) &= -\mathcal{X} - \frac{s(4m_\pi^2 - s) + 4(m_\pi^4 - tu)}{2}\mathcal{Y} . \end{aligned} \quad (12)$$

The center of mass velocity for outgoing particles  $\beta^{ab}(s)$  will be defined as

$$\beta^{ab}(s) = \sqrt{\left(1 - \frac{(m_a + m_b)^2}{s}\right) \left(1 - \frac{(m_a - m_b)^2}{s}\right)} . \quad (13)$$

### III. MASTER FORMULAE RESULT

The master formula approach to two flavours developed by two of us [17] can be readily extended to three flavours [19]. In short, the extended S-matrix with strangeness included obeys a new and linear master equation, that is emmenable to on-shell chiral reduction formulas. The fusion reaction processes can be assessed as discussed in [17,18] for two flavours. The three flavour result is

$$\begin{aligned} \mathcal{T}_1 &= i\epsilon_1 \cdot \epsilon_2 \frac{E_a}{E_b} (f^{bci} f^{ida} + f^{bdi} f^{ica}) \\ &\quad + i4\epsilon_1 \cdot k_2 \epsilon_2 \cdot k_1 \frac{E_a}{E_b} \left\{ \frac{f^{bci} f^{ida}}{u - m_i^2} + \frac{f^{bdi} f^{ica}}{t - m_i^2} \right\} \\ \mathcal{T}_2 &= i\epsilon_1 \cdot \epsilon_2 \frac{1}{E_a E_b} f^{bdi} f^{aci} \left\{ \frac{2}{3} K \frac{M_a}{m_a^2} - E_i^2 \right\} \\ &\quad + \epsilon_1^\mu \epsilon_2^\nu k_2^\beta k_1^\alpha \frac{1}{E_a E_b} \int d^4 z \int d^4 y \int d^4 x e^{ik_2 \cdot x - iq_1 \cdot y - iq_2 \cdot z} \langle T^* \mathbf{V}_\nu^d(z) \mathbf{V}_\mu^c(y) \mathbf{j}_{A\beta}^b(x) \mathbf{j}_{A\alpha}^a(0) \rangle \\ &\quad + i\epsilon_1^\mu \epsilon_2^\nu \frac{2}{3} \frac{K}{C} \delta^{ab} \frac{M_a}{E_a^2} \int d^4 z \int d^4 y e^{-iq_1 \cdot y - iq_2 \cdot z} \langle T^* \mathbf{V}_\nu^d(z) \mathbf{V}_\mu^c(y) \sigma^0(0) \rangle \\ &\quad - i\epsilon_1^\mu \epsilon_2^\nu d^{abh} \frac{M_b}{E_a E_b} \frac{E_h m_h^2}{M_h} \int d^4 z \int d^4 y e^{-iq_1 \cdot y - iq_2 \cdot z} \langle T^* \mathbf{V}_\nu^d(z) \mathbf{V}_\mu^c(y) \sigma^h(0) \rangle , \end{aligned} \quad (14)$$

where  $\mathcal{T}_1$  summarizes the Born contributions to the charged mesons, and  $\mathcal{T}_2$  the rest after two chiral reductions of the external meson states. (15) constitutes our basic identity. It shows that the fusion reaction is related to the vacuum correlators  $\mathbf{V}\mathbf{V}\mathbf{j}\mathbf{j}$  and  $\mathbf{V}\mathbf{V}\sigma$  modulo Born terms. Quantum numbers and G-parity imply that the scalars dominate the final state interactions in the s-channel. This point will become clearer in the resonance saturation analysis. What is remarkable in (15) is that the final state scalar correlations are driven by the symmetry breaking effects in QCD.

In (15) the isovector current  $\mathbf{V}$  and the one-pion reduced iso-axial current  $\mathbf{j}_A$  are given by

$$\mathbf{V}_\mu^a = \bar{q}\gamma_\mu \frac{\lambda^a}{2} q , \quad \mathbf{j}_{A\mu}^a = \bar{q}\gamma_\mu \frac{\lambda^a}{2} \gamma_5 q + \left( \frac{M}{m_p^2} \right)^{ab} \partial_\mu (\bar{q} i \gamma_5 \lambda^b q) . \quad (16)$$

The mesons weak-decay constants and masses are

$$\begin{aligned} E_{1\sim 8} &\equiv (f_\pi, f_\pi, f_\pi, f_K, f_K, f_K, f_K, f_\eta) \\ m_{1\sim 8} &\equiv (m_\pi, m_\pi, m_\pi, m_K, m_K, m_K, m_K, m_\eta) \end{aligned} \quad (17)$$

with  $f_\pi = 93$  MeV,  $f_K = 115$  MeV and  $f_\eta = 123$  MeV. The current mass matrix is chosen as

$$M_{1\sim 8} \equiv \left( \hat{m}, \hat{m}, \hat{m}, \frac{\hat{m} + m_s}{2}, \frac{\hat{m} + m_s}{2}, \frac{\hat{m} + m_s}{2}, \frac{\hat{m} + m_s}{2}, \frac{\hat{m} + 2m_s}{3} \right) \quad (18)$$

with  $\hat{m} = 9$  MeV and  $m_s = 175$  MeV for some running scale. Since the  $M$ 's appear in RGE invariant combinations, the effects of the running scale is small in the range of energies probed by the fusion reaction processes we will be considering. The scalar densities are

$$\begin{aligned}\sigma^0 &= \frac{C}{K} \bar{q}q + C \\ \sigma^h &= -\frac{M_a}{E_a m_a^2} \bar{q} \lambda^a q.\end{aligned}\quad (19)$$

with two (arbitrary) constants. For two flavours,  $C \rightarrow -f_\pi$  and  $2K/3 \rightarrow f_\pi^2 m_\pi^2 / \hat{m}$ .

The contact term in  $\mathcal{T}_2$  vanishes in the two-flavour case. It does not in the tree-flavour case and is to be reabsorbed in the pertinent counterterm generated by the three and four point functions in (15). The Born terms involve only charged mesons. Their explicit form is

$$\begin{aligned}\mathcal{T}_{\gamma\gamma \rightarrow \pi^+\pi^-} &= -i2e^2 \epsilon_1 \cdot \epsilon_2 - i4e^2 \epsilon_1 \cdot k_1 \epsilon_2 \cdot k_2 \left( \frac{1}{t - m_\pi^2} + \frac{1}{u - m_\pi^2} \right) \\ \mathcal{T}_{\gamma\gamma \rightarrow K^+K^-} &= -i2e^2 \epsilon_1 \cdot \epsilon_2 - i4e^2 \epsilon_1 \cdot k_1 \epsilon_2 \cdot k_2 \left( \frac{1}{t - m_K^2} + \frac{1}{u - m_K^2} \right).\end{aligned}\quad (20)$$

These tree results are consistent with all chiral models with minimal coupling. To go beyond, we need to assess the effects of the three- and four-point functions in (15). We will do this in two ways : at threshold by using power counting, and beyond threshold by using resonance saturation methods.

#### IV. ONE LOOP RESULT

The identity (15) is a consequence of broken chiral symmetry in QCD, and any chiral approach that is consistent with QCD ought to satisfy it. In this section we show how this identity can be analysed near threshold using power counting in  $1/E$ . A simple comparison with the nonlinear sigma model shows that this is analogous to the loop expansion if  $\phi = \mathbf{V}, \mathbf{j}_A, \sigma$  are counted of order  $\mathcal{O}(1)$ . Also  $f_K^2 - f_\pi^2$  and  $f_\eta^2 - f_\pi^2$  are  $\mathcal{O}(1)$  rather than  $\mathcal{O}(E)$  because of G-parity.

Some details regarding the one-loop analysis are given in Appendix B. The results for the various transition amplitudes are

$$\begin{aligned}\mathcal{T}_{\gamma\gamma \rightarrow \pi^+\pi^-} &= -i2e^2 k_1 \cdot k_2 \frac{1}{f_\pi^2} \left( \tilde{\mathcal{I}}^\pi + \frac{1}{2} \tilde{\mathcal{I}}^K \right) - i2e^2 \frac{m_\pi^2}{f_\pi^2} \tilde{\mathcal{I}}^\pi - ie^2 \frac{m_K^2}{f_\pi^2} \frac{2\hat{m}}{\hat{m} + m_s} \tilde{\mathcal{I}}^K \\ \mathcal{T}_{\gamma\gamma \rightarrow \pi^0\pi^0} &= -i2e^2 k_1 \cdot k_2 \frac{1}{f_\pi^2} \left( 2\tilde{\mathcal{I}}^\pi + \frac{1}{2} \tilde{\mathcal{I}}^K \right) - i2e^2 \frac{m_\pi^2}{f_\pi^2} \tilde{\mathcal{I}}^\pi - ie^2 \frac{m_K^2}{f_\pi^2} \frac{2\hat{m}}{\hat{m} + m_s} \tilde{\mathcal{I}}^K \\ \mathcal{T}_{\gamma\gamma \rightarrow K^+K^-} &= -i2e^2 k_1 \cdot k_2 \frac{1}{f_K^2} \left( \frac{1}{2} \tilde{\mathcal{I}}^\pi + \tilde{\mathcal{I}}^K \right) - ie^2 \frac{m_\pi^2}{f_K^2} \frac{\hat{m} + m_s}{2\hat{m}} \tilde{\mathcal{I}}^\pi - i\frac{3}{2} e^2 \frac{m_K^2}{f_K^2} \tilde{\mathcal{I}}^K \\ \mathcal{T}_{\gamma\gamma \rightarrow K^0\bar{K}^0} &= -i2e^2 k_1 \cdot k_2 \frac{1}{f_K^2} \left( \frac{1}{2} \tilde{\mathcal{I}}^\pi + \frac{1}{2} \tilde{\mathcal{I}}^K \right) - ie^2 \frac{m_\pi^2}{f_K^2} \frac{\hat{m} + m_s}{2\hat{m}} \tilde{\mathcal{I}}^\pi - i\frac{3}{2} e^2 \frac{m_K^2}{f_K^2} \tilde{\mathcal{I}}^K \\ \mathcal{T}_{\gamma\gamma \rightarrow \eta\eta} &= -i3e^2 k_1 \cdot k_2 \frac{1}{f_\eta^2} \tilde{\mathcal{I}}^K - i\frac{2}{3} e^2 \frac{m_\pi^2}{f_\eta^2} \frac{\hat{m} + 2m_s}{3\hat{m}} \tilde{\mathcal{I}}^\pi - i\frac{5}{3} e^2 \frac{m_K^2}{f_\eta^2} \frac{2(\hat{m} + 2m_s)}{3(\hat{m} + m_s)} \tilde{\mathcal{I}}^K \\ \mathcal{T}_{\gamma\gamma \rightarrow \pi^0\eta} &= -i\sqrt{3}e^2 k_1 \cdot k_2 \frac{1}{f_\pi f_\eta} \tilde{\mathcal{I}}^K\end{aligned}\quad (21)$$

with  $k_1 \cdot k_2 = \frac{1}{2}(s - m_1^2 - m_2^2)$ . The one-loop finite contributions are

$$\begin{aligned}\tilde{\mathcal{I}}^i &\equiv -H(s - 4m_i^2) \epsilon_1 \cdot \epsilon_2 \frac{1}{16\pi^2} \left\{ 1 + \frac{m_i^2}{s} \left( \ln \left[ \frac{\sqrt{s} - \sqrt{s - 4m_i^2}}{\sqrt{s} + \sqrt{s - 4m_i^2}} \right] + i\pi \right)^2 \right\} \\ &\quad - H(4m_i^2 - s) \epsilon_1 \cdot \epsilon_2 \frac{1}{16\pi^2} \left\{ 1 - \frac{4m_i^2}{s} \arctan \sqrt{\frac{s}{4m_i^2 - s}} \right\},\end{aligned}\quad (22)$$

where  $H(x)$  is the Heaviside function. Following [17] we used the LHZ subtraction procedure. The ensuing counterterms (one) are fixed by electric charge conservation. The results are independent of the parameters  $C$  and  $K$  introduced in (19). They are also in agreement with one-loop chiral perturbation theory (ChPT) [15] modulo counterterms. In ChPT all possible counterterms commensurate with symmetry and power counting are retained, in our case only those that show up in the loop expansion (minimal). Which of which is relevant is only determined by comparison with (threshold) experiments. Below, we will show that both procedures yield almost identical results.

## V. RESONANCE SATURATION RESULT

To be able to address the fusion reaction processes beyond threshold we need to take into account the final state interactions in (15). One way to do this is to use dispersion analysis for the three- and four-point functions with minimal weight-insertions. This is equivalent to a tree-level resonance saturation of the three- and four-point functions as shown in Fig. 1 with all possible crossings. Note that contact interactions are covered by the present description in the limit where the masses of the  $\sigma$ ,  $V$  and  $A$  are taken to be very large.

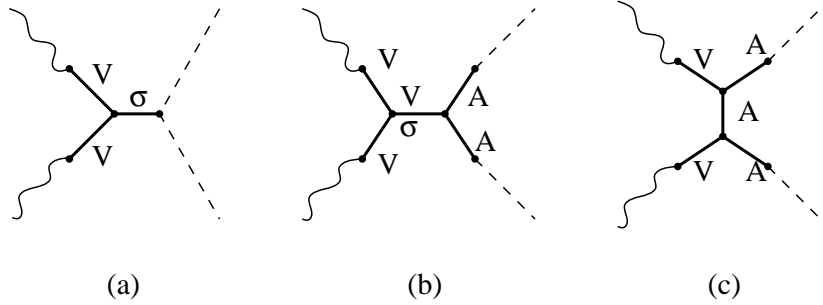


FIG. 1. Diagram for  $\langle \mathbf{V}\mathbf{V}\sigma \rangle$  (a) and  $\langle \mathbf{V}\mathbf{V}\mathbf{j}_A\mathbf{j}_A \rangle$  (b,c).

From quantum numbers and parity, the vector current  $\mathbf{V}_\mu^a$  will be saturated by the light vector mesons ( $v_\mu^a = \rho, \omega, \phi$ ), and the one-pion reduced axial-vector current  $\mathbf{j}_{A\mu}^a$  by the light axial-vector mesons ( $a_\mu^a = A_1, K_1$ ) [19]. Typically,

$$\begin{aligned} \langle 0 | \mathbf{V}_\mu^a(x) | v_\nu^b(p) \rangle &\sim g_{\mu\nu} \delta^{ab} \epsilon_\mu^V f_{v_a} m_{v_a} e^{-ip \cdot x} \\ \langle 0 | \mathbf{j}_{A\mu}^a(x) | a_\nu^b(p) \rangle &\sim g_{\mu\nu} \delta^{ab} \epsilon_\mu^A f_{a_a} m_{a_a} e^{-ip \cdot x} . \end{aligned} \quad (23)$$

Since the photon carries indices  $c, d = 3, 8$

$$\begin{aligned} v^3 &= \rho^0 \\ v^8 &= \sqrt{\frac{1}{3}} \omega^0 - \sqrt{\frac{2}{3}} \phi , \end{aligned} \quad (24)$$

only the chargeless vector mesons contribute to the fusion process. The occurrence of the structure constant  $f^{abc}$  in the reduction of the fusion reaction forces the axial-vector mesons to carry indices 3, 8 as well. Hence, only  $a^{1,2} = A_1$  and  $a^{4 \sim 7} = K_1$  will be needed in our case.

Similarly for  $\mathbf{V}\mathbf{V}\mathbf{j}_A\mathbf{j}_A$  with

$$\langle 0 | \mathbf{V}_\mu^d \mathbf{V}_\nu^c \mathbf{j}_A^b \mathbf{j}_A^a | 0 \rangle = \epsilon_\mu^V \epsilon_\nu^V \epsilon_\delta^A \epsilon_\gamma^A f_{a_a} f_{a_b} f_{v_c} f_{v_d} m_{a_a} m_{a_b} m_{v_c} m_{v_d} \langle 0 | v_\mu^d v_\nu^c a_\delta^b a_\gamma^a | 0 \rangle . \quad (25)$$

Finally, the scalar field  $\hat{\sigma}$  can be saturated by scalar mesons giving  $\mathbf{V}\mathbf{V}\sigma$  as

$$\langle \mathbf{V}_\mu^d \mathbf{V}_\nu^c \hat{\sigma} \rangle = \epsilon_\mu^V \epsilon_\nu^V f_{v_c} f_{v_d} m_{v_c} m_{v_d} \langle v_\mu^d v_\nu^c \sigma \rangle . \quad (26)$$

All the mesons will have masses and widths fixed at their PDG (Particle Data Group) values.

With the above in mind the various contributions from Fig. 1 can be readily constructed. In Appendix C we show how they could also be retrieved using a linear sigma-model. The contribution to  $\mathbf{V}\mathbf{V}\sigma$  is

$$\mathcal{T}_{vv\sigma}^{ab} = 4ie^2 \left( c_0 \delta^{ab} \delta^{cd} \delta^{h0} + c_h d^{abh} d^{cdh} \right) \epsilon_1 \cdot \epsilon_2 \frac{\Lambda M_b}{E_a E_b} \frac{f_{v_c} f_{v_d}}{m_{v_c} m_{v_d}} \frac{1}{s - m_{\sigma_h}^2} . \quad (27)$$

The insertions of powers of  $1/E$  and the scale  $\Lambda$  ( $= 1$  GeV) are to make the arbitrary parameters  $c_h$  (two) dimensionless. They will be fixed by threshold constraints. The scalar contribution to  $\mathbf{VVj}_{AJA}$  is

$$\begin{aligned} \mathcal{T}_{vva\sigma_0}^{ab} = & i16e^2 (g_1 \delta^{cd} \delta^{ab} \delta^{h0} + g_2 d^{cdh} d^{abh}) \epsilon_1 \cdot \epsilon_2 \frac{\Lambda^2}{E_a E_b} \frac{f_{v_c} f_{v_d}}{m_{v_c} m_{v_d}} \frac{1}{s - m_{\sigma_h}^2} \\ & \times k_1 \cdot k_2 \left( 1 - \frac{m_a^2}{m_{a_a}^2} - \frac{m_b^2}{m_{a_b}^2} + \frac{m_a^2}{m_{a_a}^2} \frac{m_b^2}{m_{a_b}^2} \right) \frac{f_{a_a} m_{a_a}}{m_a^2 - m_{a_a}^2} \frac{f_{a_b} m_{a_b}}{m_b^2 - m_{a_b}^2}. \end{aligned} \quad (28)$$

The dimensionless parameters  $g_h$  (two) are again arbitrary. The intermediate vector contribution from Fig. 1-(b) vanishes because of the antisymmetry of the structure constant  $f^{abc}$ . Finally, the contribution from Fig. 1-(c) is

$$\begin{aligned} \mathcal{T}_{vva\sigma_0}^{ab} = & -i16e^2 g_3 f^{caf} f^{dbf} \frac{1}{E_a E_b} \left( \frac{f_{v_c} f_{v_d}}{m_{v_c} m_{v_d}} \right) \left( \frac{1}{t - m_{a_f}^2} \right) \left( \frac{f_{a_a} m_{a_a}}{m_a^2 - m_{a_a}^2} \right) \left( \frac{f_{a_b} m_{a_b}}{m_b^2 - m_{a_b}^2} \right) \\ & \times \left[ (\epsilon_1 \cdot k_1)(\epsilon_2 \cdot k_2) \left( 1 - \frac{t}{m_{a_f}^2} \right) \left( -t + m_a^2 + m_b^2 - \frac{(k_1 \cdot q_1)^2}{m_{a_a}^2} - \frac{(k_2 \cdot q_2)^2}{m_{a_b}^2} \right) \right. \\ & \left. + \left( \epsilon_1 \cdot \epsilon_2 + \frac{(\epsilon_1 \cdot k_1)(\epsilon_2 \cdot k_2)}{m_{a_f}^2} \right) \left( m_a^2 - \frac{(k_1 \cdot q_1)^2}{m_{a_a}^2} \right) \left( m_b^2 - \frac{(k_2 \cdot q_2)^2}{m_{a_b}^2} \right) \right] \\ & + (t, a, k_1 \leftrightarrow u, b, k_2) \end{aligned} \quad (29)$$

with one additional dimensionless parameter  $g_3$ .

In the vector and axial channels all the resonances quoted above are introduced with their masses and decay widths in the form of Breit-Wigner resonances fixed at their PDG values. In the scalar channels we will use three resonances for  $\sigma^0$ :  $f_0(500)$ ,  $f_0(980)$  and  $f_2(1270)$ . As our chief goal is to test the master formula result with resonance saturation, we will keep our description simple by substituting

$$\frac{1}{s - m_{\sigma_0}^2} \rightarrow \sum_{m_f} \frac{f_f}{s - m_f^2 + iG(s, m_f)m_f} \quad (30)$$

with  $f_{f_0(500)} = f_{f_2(1270)} = 1$  and  $f_{f_0(980)} = 0.05$ , and the decay widths

$$G(s, m_f) = H(s - 4m_\pi^2) G_0 \left( \frac{1 - 4m_\pi^2/s}{1 - 4m_\pi^2/m_f^2} \right)^n, \quad (31)$$

with  $n = 1/2$  and  $3/2$  for scalar and vector mesons, respectively. A more detailed parametrization of the partial widths and so on will not be attempted here, again for simplicity. We have found that the contribution of  $f_0(980)$  is suppressed (hence the order of magnitude change in the weight) in agreement with previous investigations [16]. In the numerical analysis to follow, we have checked that our results are not greatly sensitive to the resonance parametrizations provided that PDG masses and widths are enforced.

In the isotriplet-scalar channel  $\sigma^3$  we have:  $a_0(980)$  and  $a_2(1320)$ , giving

$$\frac{1}{s - m_{\sigma_3}^2} \rightarrow \frac{0.6}{s - m_{a_0}^2 + iG_{a_0}(s)m_{a_0}} - \frac{1}{s - m_{a_2}^2 + iG_{a_2}(s)m_{a_2}}. \quad (32)$$

The same functional form for  $G$  is used, but with a different cut-off corresponding to the lowest mass yields in the various decay channels. The relative sign in (32) reflects the attractive character of  $a_2(1320)$  in comparison to  $a_0(980)$  in the isotriplet channel. We will not consider the effects of  $\sigma^8$  as it involves higher octet-scalar resonances.

## VI. POLARIZABILITIES

Before discussing in details how our analysis of the fusion reactions compare in details to the present data, we will first address the issue of the meson polarizabilities as inferred from our one-loop analysis. For the charged pions [11],

$$\begin{aligned} \bar{\alpha}_E^{\pi^\pm} &= (6.8 \pm 1.4 \pm 1.2) \times 10^{-4} \text{ fm}^3 \\ \bar{\alpha}_E^{\pi^\pm} &= (20 \pm 12) \times 10^{-4} \text{ fm}^3 \\ \bar{\alpha}_E^{\pi^\pm} &= (2.2 \pm 1.6) \times 10^{-4} \text{ fm}^3, \end{aligned} \quad (33)$$

and for the neutral pions [11]

$$\begin{aligned} |\bar{\alpha}_E^{\pi^0}| &= (0.69 \pm 0.07 \pm 0.04) \times 10^{-4} \text{ fm}^3 \\ |\bar{\alpha}_E^{\pi^0}| &= (0.8 \pm 2.0) \times 10^{-4} \text{ fm}^3 . \end{aligned} \quad (34)$$

The data are not accurate enough. This notwithstanding, our one-loop result for the charged pions is

$$\alpha_L^{\pi^\pm} \approx 4.2 \times 10^{-4} \text{ fm}^3 , \quad (35)$$

this is twice the value obtained using standard chiral perturbation theory [11]. The difference stems for the additional (finite) counterterms in ChPT, which are purposely absent (minimal) in our analysis. This point was discussed in great details in [17]. For the neutral pions we have

$$\alpha_L^{\pi^0} \approx 6.3 \times 10^{-4} \text{ fm}^3 . \quad (36)$$

For the rest of the octet, we have

$$\begin{aligned} \alpha_L^{K^\pm} &\approx -2.7 \times 10^{-5} \text{ fm}^3 \\ \alpha_L^{K^0 \bar{K}^0} &\approx +2.8 \times 10^{-5} \text{ fm}^3 \\ \alpha_L^\eta &\approx -4.4 \times 10^{-6} \text{ fm}^3 . \end{aligned} \quad (37)$$

In the resonance saturation approach, the polarizabilities follow essentially from the  $\mathbf{V}\mathbf{V}\mathbf{j}_A\mathbf{j}_A$  contributions in (29). These contributions are constrained at high energy to be small, resulting into naturally small polarizabilities. A global fit yields pion polarizabilities that are similar for charged and chargeless fusion reactions.

## VII. NUMERICAL RESULTS

Most of the calculations to be discussed in this section are carried with the PDG parameters for the quoted resonances. The dimensionless couplings involved in the resonance saturation approach are chosen so as to give a global fit that is consistent with the threshold constraints (mainly one-loop). Specifically, we will use

$$\begin{aligned} c_0 &= -98208 \\ c_3 &= 5c_0 \\ g_1 &= 0.9744 \\ g_2 &= -13.64 \\ g_3 &= -1.5 , \end{aligned} \quad (38)$$

with  $c_8 = 0$  since we are ignoring the effects from  $\sigma^8$ . Some of the results for the total cross sections to be quoted will involve a parameter  $Z$  defined as

$$\sigma_Z = 2 \int_0^Z d\cos\theta \frac{d\sigma}{d\cos\theta} \quad (39)$$

where  $\theta$  is the relative angle between one of the two incoming photons and the outgoing mesons.

### A. Pions

In Fig. 2 we show the total cross section for fusion to charged pions up to  $Z = 0.6$ . The data are from [1–4]. The overall agreement with the data is good. Our analysis appears to favor the SLAC-PEP-MARK-II as well as the KEK-TE-001 data. The peak at  $f_2(1270)$  is clearly visible, while the  $f_0(980)$  is weaker. The Born contribution overwhelms the  $f_0(500)$  contribution in this channel, and is hardly visible in our results as well as the data. In the insert, we show an enlargement of the threshold region and comparison with our Born contribution, the one-loop analysis, and the resonance saturation approach. Overall, our approximations are consistent.

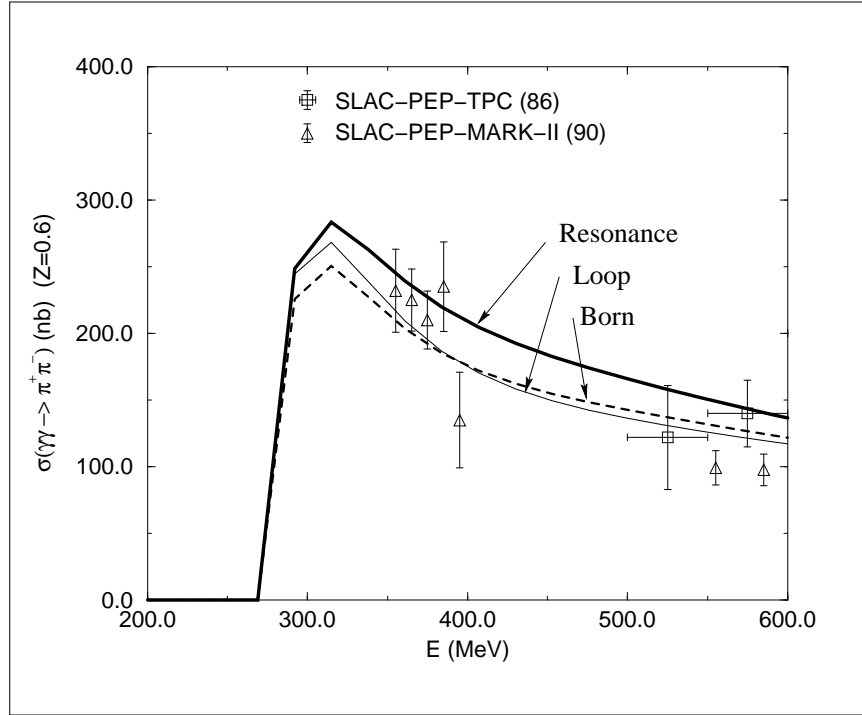
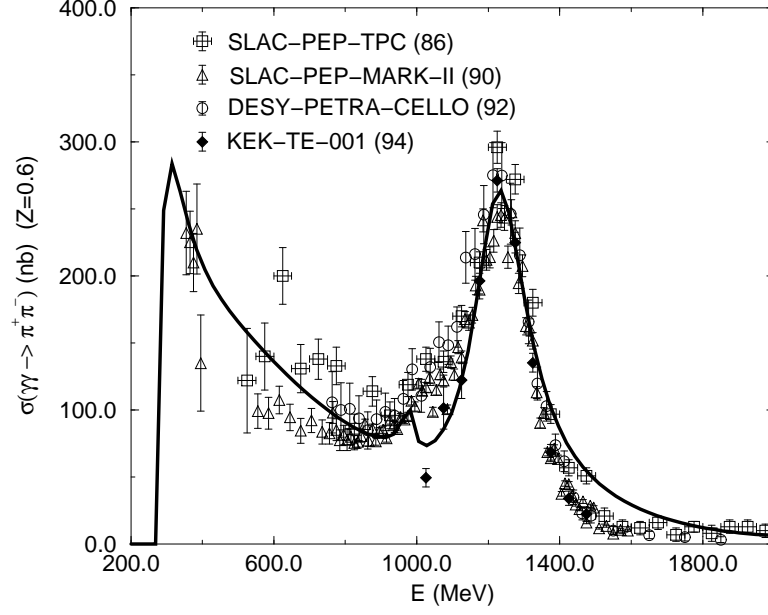


FIG. 2. Total cross section for  $\gamma\gamma \rightarrow \pi^+\pi^-$  ( $Z = 0.6$ ). Thick (thin) line correspond to resonance (loop) contribution. Dashed line in the lower panel corresponds to the Born term. The data are collected from Refs. [1–4]

In Fig. 3 we present our results for the fusion reaction into chargeless pions with  $Z = 0.8$ . The data are from [5,6]. Again the  $f_2(1270)$  is clearly visible, while the  $f_0(980)$  is barely. The broad effects from the  $f_0(500)$  are also visible in comparison to the data. The resonance saturation result is in overall agreement with the both sets of data. In the insert, we show an enlargement of the threshold region and comparison to our one-loop result as well as one-loop and two-loop ChPT. Clearly our one-loop and the one-loop ChPT are in good agreement although our construction is minimal (fewer counterterms). Most of the parameters (six) in the two-loop results from ChPT are fit using ideas similar to the resonance saturation approach we have adopted.



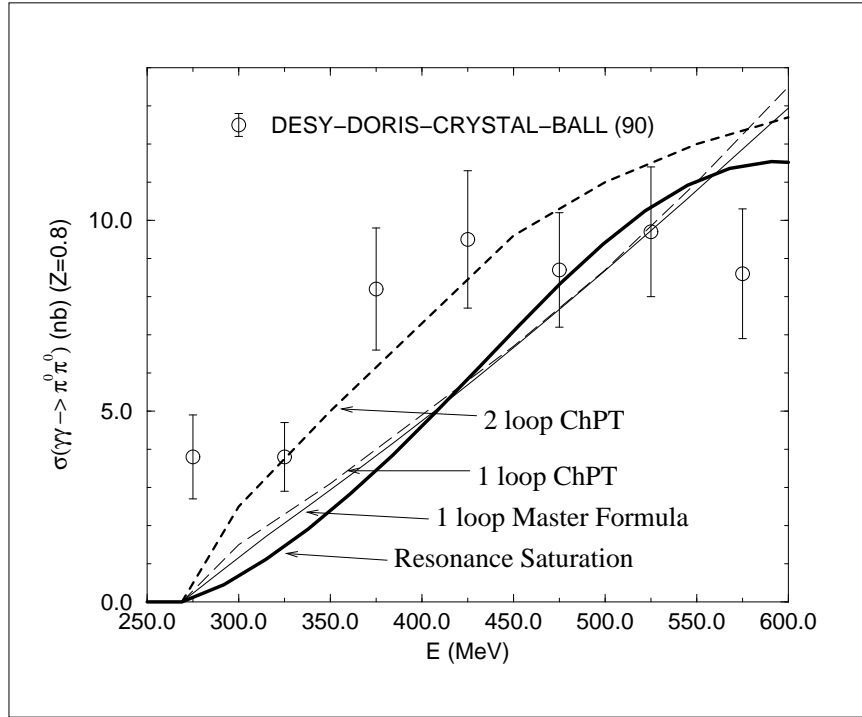
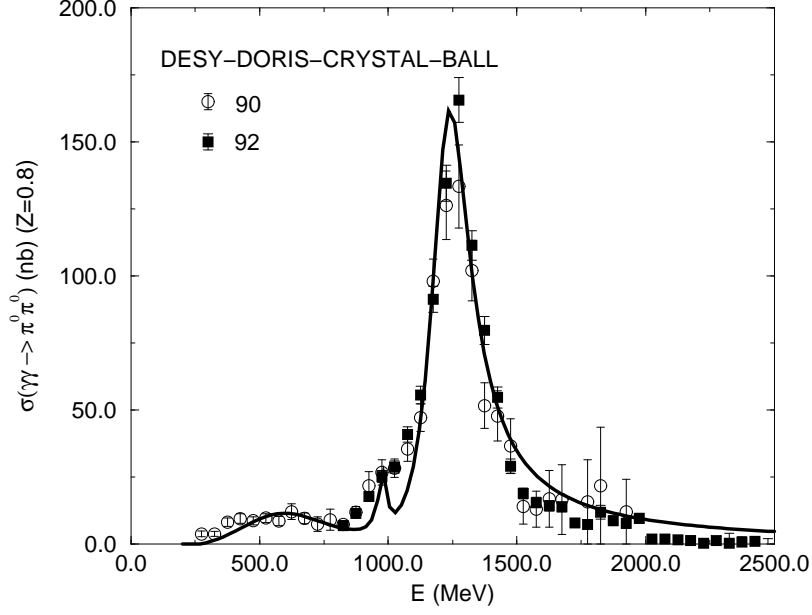


FIG. 3. Total cross section for  $\gamma\gamma \rightarrow \pi^0\pi^0$  ( $Z = 0.8$ ). Thick (thin) line correspond to resonance (loop) contribution. The dashed lines in the lower panel are the 1- and 2-loop ChPT results [15]. The data are taken from Refs. [5,6].

### B. Kaons

In Fig. 4 we present our results for the fusion reaction into charged kaons. For  $Z = 0.6$  our analysis shows a threshold enhancement at about 980 MeV, followed by another enhancement at  $a_2(1320)$ . The enhancement shown in the SLAC-PEP-TCP data is consistent with the  $a_2(1320)$ , although the error bars are large. Our results for the cross section are higher than the data in the energy range  $\sqrt{s} = 1.6 - 2.4$  GeV. For  $Z = 1.0$  we compare the resonance

saturation results with the Born amplitude and the one-loop approximation. Again we see the same features as those encountered at  $Z = 0.6$ . The DESY-DORIS-ARGUS data agree with our analysis around the  $a_2(1320)$ , but are not in agreement at threshold and above  $\sqrt{s} = 1.6$  GeV. The threshold enhancement due to the Born terms in our analysis is only partly decreased by the repulsive character of the scalar-isotriplet  $a_0(980)$ . A similar behaviour was also noted by Oller and Oset [16] using a coupled channel analysis.

In Fig. 5 we show our results for chargeless kaons. Our results favor the data from DESY-PETRA-CELLO [9] as opposed to the early data from DESY-PETRA-TASSO [8], although the data have large error bars. The effects from the  $a_0(980)$  is weaker than the one from the  $a_2(1320)$ . In this case the Born contribution vanishes.

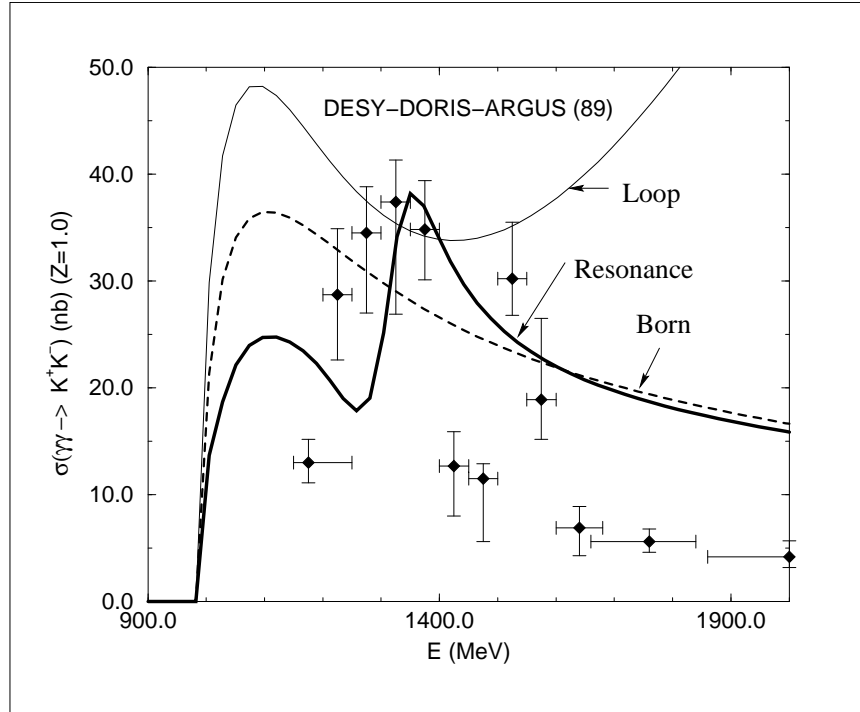
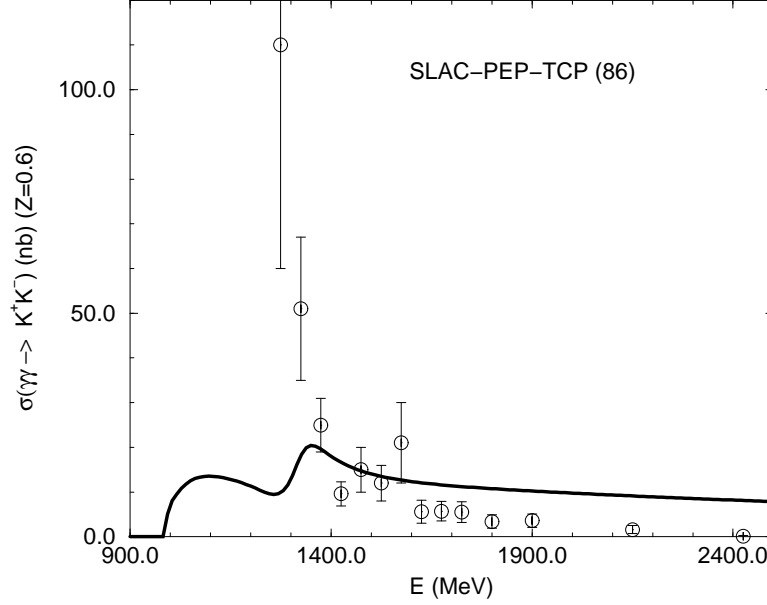


FIG. 4. Total cross section for  $\gamma\gamma \rightarrow K^+K^-$  with  $Z=0.6$  and  $Z=1.0$ . Thick (thin) line corresponds to resonance (loop) contribution. The Born terms are plotted as dashed line. The data are taken from Refs. [1,7].

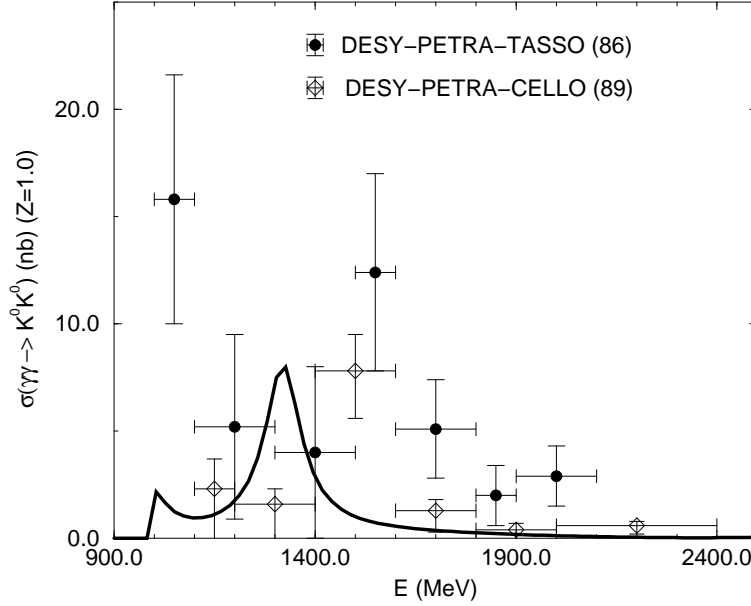


FIG. 5. Total cross section for  $\gamma\gamma \rightarrow K^0\bar{K}^0$  ( $Z=1.0$ ). The data are taken from Refs. [8,9].

### C. Etas

In Fig. 6 we show our results for the fusion into  $\pi^0\eta$  for  $Z = 0.9$ . The peaks are the scalar-isotriplets  $a_0(980)$  and  $a_2(1320)$ . There is fair agreement with the DESY-DORIS-CRYSTAL-BALL [10] data. The strength between the two-resonances follow simply from the relative sign in (32) reflecting on the attraction-repulsion in these two channels. In Fig. 7 we show our predictions for the fusion reaction to two eta's. The cross section is tiny in comparison to the other fusion reactions (about four orders of magnitude down). The reason is the near cancellation between the  $f_2(1270)$  contribution in  $\mathbf{VV}\sigma$  and  $\mathbf{VVj_Aj_A}$  ( $c_0$  and  $g_1$  have opposite signs). Since the resonance is smeared differently in the two contributions, the exact cancellation takes place in the range  $1.25 - 1.5$  GeV.

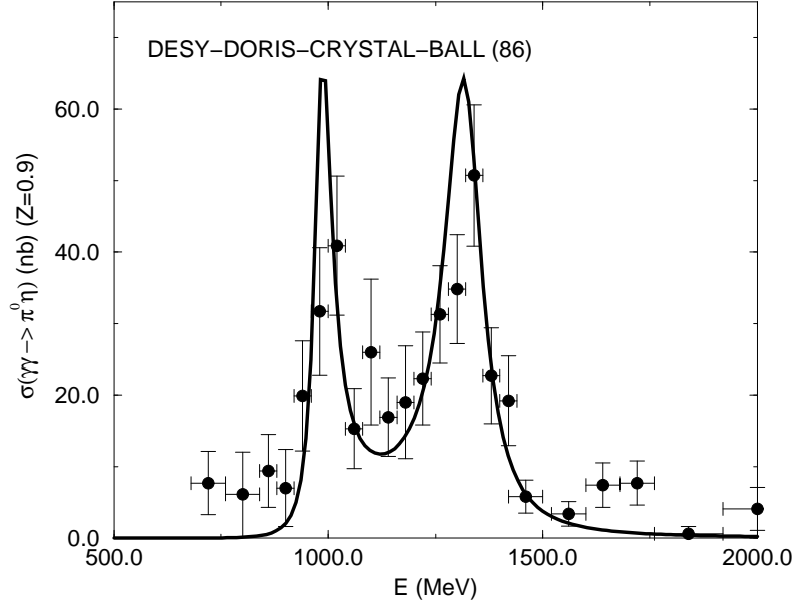


FIG. 6. Total cross section for  $\gamma\gamma \rightarrow \pi^0 \eta$  ( $Z=0.9$ ). The data are taken from Refs. [10].

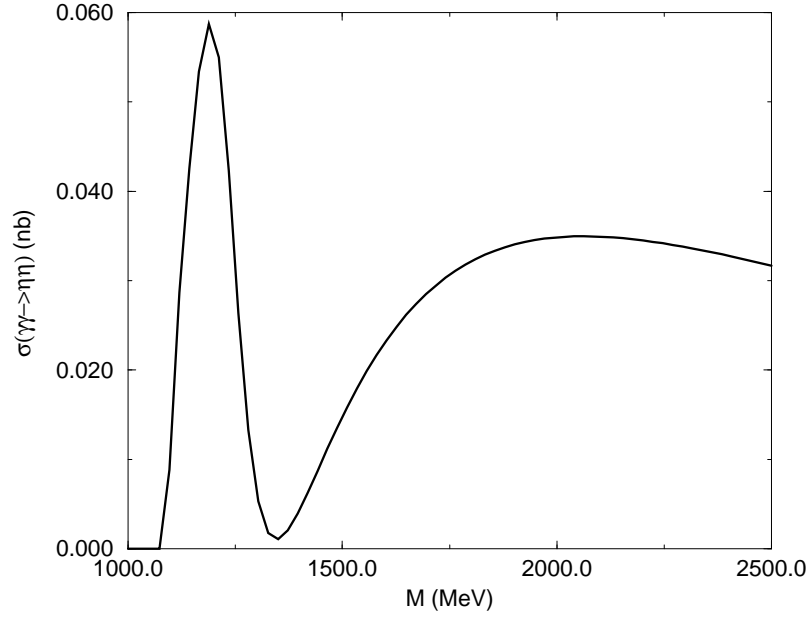


FIG. 7. Total cross section for  $\gamma\gamma \rightarrow \eta\eta$ .

## VIII. CONCLUSIONS

We have analyzed the two-photon fusion reaction to two mesons using the master formulae approach to QCD with three flavors. The formulae for the fusion reaction amplitude encodes all the information about chiral symmetry and its breaking in QCD. We have analyzed this result in power counting and shown that it is overall in agreement with results from three-flavor ChPT in the threshold region. We have derived specific results for the real part of the polarizabilities of all the octet mesons.

To analyze the reactions beyond threshold, we have implemented a simple dispersion analysis on the pertinent three- and four-point functions in the form of tree-level resonance saturation. The analysis enforces broken chiral symmetry, unitarity and crossing symmetry in a straightforward way. The pertinent resonance parameters (masses and widths) are fixed at their PDG values. Their couplings result into 5 parameters which we use to globally fit all available data through  $\sqrt{s} = 2$  GeV and predict a very small cross section for  $\gamma\gamma \rightarrow \eta\eta$ .

The master formulae to the fusion reaction processes implies from first principles scalar-isoscalar and scalar-isotriplet correlations in the s-channel, and axial-vector correlations in t-channels. The latter enforce the correct polarizabilities, while the former account for most of the resonances seen in the experiments. In particular, the scalar-isoscalar  $f_0(500)$ ,  $f_0(980)$  and  $f_2(1270)$  are predominant in the fusion reactions involving pions, while the scalar-isotriplet  $a_0(980)$  and  $a_2(1320)$  are important in the fusion reactions involving kaons, and also etas and pions. The  $a_0(980)$  is found to decrease considerably the threshold enhancements caused by the Born term in the fusion to charged kaons, in agreement with present experiments. The present results are important in the assessment of the electromagnetic emission rates from a hadronic gas in relativistic heavy-ion collisions [20].

## ACKNOWLEDGEMENT

IZ would like to thank Jose Oller and Eulogio Oset for discussions. This work was supported by the U.S. Department of Energy under Grant No. DE-FG02-88ER40388.

- 
- [1] H. Aihara et al., Phys. Rev. Lett. 57 (1986) 404.
  - [2] J. Boyer et al., Phys. Rev. D42 (1990) 1350.
  - [3] H.-J. Behrend et al., Z. Phys. C56 (1992) 381.
  - [4] Yabuki, KEK-PREPRINT-94-183.
  - [5] H. Marsiske et al., Phys. Rev. D41 (1990) 3324.
  - [6] Bienlein, Proceedings of San Diego Workshop (1992).
  - [7] H. Albrecht et al., Z. Phys. C48 (1989) 183.
  - [8] M. Althoff et al., Z. Phys. C29 (1986) 189.
  - [9] H.-J. Behrend et al., Z. Phys. C43 (1989) 91.
  - [10] D. Antreasyan et al., Phys. Rev. D33 (1986) 1847.
  - [11] J. F. Donoghue and B. R. Holstein, Phys. Rev. D 48 (1993) 137.
  - [12] D. Morgand and M.R. Pennington, Phys. Lett. B 272 (1991) 134;  
T.N. Truong, Phys. Lett. B 313 (1993) 221.
  - [13] P. Ko, Phys. Rev. D 41 (1990) 1531.
  - [14] J. Bijnens and F. Cornet, Nucl. Phys. B 296 (1988) 557;  
J.F. Donoghue, B.R. Holstein and Y.C. Lin, Phys. Rev. D 37 (1988) 2423.
  - [15] S. Bellucci, J. Gasser, M.E. Sainio, Nucl. Phys. B 423 (1994) 80.
  - [16] J.A. Oller and E. Oset, Nucl. Phys. **A 629** (1998) 739, and references therein.
  - [17] H. Yamagishi and I. Zahed, Ann. Phys. 247 (1996) 292;  
H. Yamagishi and I. Zahed, Phys. Rev. D 53 (1996) 2288.
  - [18] S. Chernyshev and I. Zahed, SUNY-NTG-95-44, hep-ph/9511271; unpublished.
  - [19] C.H. Lee, H. Yamagishi, and I. Zahed, to be published.
  - [20] C.H. Lee, H. Yamagishi and I. Zahed, hep-ph/9806391

## IX. APPENDIX A : DETAILS OF THE BORN CONTRIBUTIONS

In this Appendix we detail the Born contributions to the T-matrix for the fusion process as given by (14-15). If we recall that the meson indices are  $(a, b)$  and the photon indices  $(c, d)$ , then the contact contributions in (14) are

$$\begin{aligned}\mathcal{T}_{11} &= ig_{\mu\nu}(E)^a(E^{-1})^b(f^{bci}f^{ida} + f^{bdi}f^{ica}) \\ &= i2\epsilon_1 \cdot \epsilon_2(E)^a(E^{-1})^b \left( f^{b3i} + \frac{1}{\sqrt{3}}f^{b8i} \right) \left( f^{ai3} + \frac{1}{\sqrt{3}}f^{ai8} \right) \\ &= -i2\epsilon_1 \cdot \epsilon_2 \times \begin{pmatrix} \pi^\pm & : & 1 \\ \pi^0 & : & 0 \\ K^\pm & : & 1 \\ \bar{K}^0 & : & 0 \\ \eta & : & 0 \end{pmatrix},\end{aligned}\tag{A.1}$$

while the pole terms are

$$\begin{aligned}\mathcal{T}_{12} &= i(2k_2 - q_1)^\mu(2k_1 - q_2)^\nu(E)^a(E^{-1})^b \left\{ f^{bci}f^{ida} \frac{1}{(k_2 - q_1)^2 - m_i^2} + f^{bdi}f^{ica} \frac{1}{(k_2 - q_2)^2 - m_i^2} \right\} \\ &= 4i\epsilon_1 \cdot k_1\epsilon_2 \cdot k_2(E)^a(E^{-1})^b \left( f^{b3i} + \frac{1}{\sqrt{3}}f^{b8i} \right) \left( f^{ai3} + \frac{1}{\sqrt{3}}f^{ai8} \right) \left( \frac{1}{u - m_i^2} + \frac{1}{t - m_i^2} \right) \\ &= -4i\epsilon_1 \cdot k_1\epsilon_2 \cdot k_2 \times \begin{pmatrix} \pi^\pm & : & [(t - m_\pi^2)^{-1} + (u - m_\pi^2)^{-1}] \\ \pi^0 & : & 0 \\ K^\pm & : & [(t - m_K^2)^{-1} + (u - m_K^2)^{-1}] \\ \bar{K}^0 & : & 0 \\ \eta & : & 0 \end{pmatrix}\end{aligned}\tag{A.2}$$

with  $q \cdot \epsilon = 0$ . Only the charged contributions appear in the Born approximation, since photons do not couple to chargeless particles at tree level. We note that the contact term in (15) contributes

$$\begin{aligned}\mathcal{T}_{21} &= ig_{\mu\nu} \frac{1}{E^a E^b} f^{bdi}f^{aci} \left\{ \frac{2}{3}K \left( \frac{M}{m_p^2} \right)^a - E_i^2 \right\} \\ &= -i2\epsilon_1 \cdot \epsilon_2 \frac{1}{E^a E^b} \left\{ \frac{2}{3}K \left( \frac{M}{m_p^2} \right)^a - E_i^2 \right\} \left( f^{b3i} + \frac{1}{\sqrt{3}}f^{b8i} \right) \left( f^{ai3} + \frac{1}{\sqrt{3}}f^{ai8} \right) \\ &= -i2\epsilon_1 \cdot \epsilon_2 \left\{ 1 - \frac{2}{3}K \left( \frac{M}{E^2 m_p^2} \right)^{\pi^\pm, K^\pm} \right\}.\end{aligned}\tag{A.3}$$

In the SU(2) case we have  $2K/3 \rightarrow (f_\pi^2 m_\pi^2)/\hat{m}$ , and this extra contribution vanishes. In the SU(3) case this extra term is of order  $1/E^2$  in power counting. It renormalizes to zero when combined with the counterterms in  $\langle \mathbf{V}\mathbf{V}\hat{\sigma} \rangle$  and  $\langle \mathbf{V}\mathbf{V}\mathbf{j}_{A\mathbf{j}_A} \rangle$ , leaving the octet charges integer-valued.

## APPENDIX B : DETAILS OF THE ONE LOOP CONTRIBUTIONS

In this Appendix we give some details regarding the one-loop analysis carried in section IV, following the discussion in [17]. In particular, we will assess the one-loop contribution to the three- and four-point correlators  $\langle \mathbf{V}\mathbf{V}\sigma \rangle$  and  $\langle \mathbf{V}\mathbf{V}\mathbf{j}_{A\mathbf{j}_A} \rangle$ .

### B-i. $\mathbf{V}\mathbf{V}\sigma$

The one-loop contribution to  $\mathbf{V}\mathbf{V}\sigma^{0,3,8}$  is generically of the form

$$\begin{aligned}\langle 0|T^*\mathbf{V}_\mu^c(x)\mathbf{V}_\nu^d(y)\hat{\sigma}_h(z)|0\rangle_{\text{con.}} &= \left[ \frac{\delta \mathbf{K}^{ii}}{\delta Y^h} \right] f^{ijc}f^{ijd} \left( g_{\mu\nu}\delta^4(x-y) \int_q e^{-iq \cdot (y-z)} \mathcal{I}^{ii}(q) \right. \\ &\quad \left. + \int_p \int_q e^{iq \cdot x - iq \cdot y - i(q-p) \cdot z} \mathcal{I}_{\mu\nu}^{ij}(q, p) \right),\end{aligned}\tag{B.1}$$

with  $(c, d) = (3, 8)$ ,  $\int_q \equiv \int d^4 q / (2\pi)^4$ , and  $\mathbf{K}$  is the  $\text{SU}(3)$  version of (3.39) in Ref. [17]. Specifically,

$$\mathbf{K}^{ac} = 2\underline{v}_\mu^{ac} \partial^\mu + \partial^\mu \underline{v}_\mu^{ac} + \underline{v}^{\mu ab} \underline{v}_\mu^{bc} - \underline{a}^{\mu ab} \underline{a}_\mu^{bc} - \frac{C}{K} Y^0 \left( \frac{m_p^2}{M} \right)^{ac} + Y^b \hat{d}^{abd} (E^{-1})^{dc}, \quad (\text{B.2})$$

with  $\underline{A}_\mu^{ac} = A_\mu^b f^{abc}$  and

$$\hat{d}^{abc} = d^{abc} \left( \frac{M}{Em_p^2} \right)^b \left( \frac{Em_p^2}{M} \right)^c. \quad (\text{B.3})$$

Here the " $\sigma^3$ " contribution vanishes because the  $K^\pm$  and  $K^{0,\bar{0}}$  contribution cancel within the loop.

The one-loop integrals are

$$\begin{aligned} \mathcal{I}^{ij}(q) &= -i \int_k \left( \frac{1}{k^2 - m_j^2 + i0} \cdot \frac{1}{(k+q)^2 - m_i^2 + i0} - (q=0) \right) \\ \mathcal{I}_{\mu\nu}^{ij}(q, p) &= i \int_k \left( \frac{1}{k^2 - m_j^2 + i0} \cdot \frac{(2k+q)_\mu}{(k+q)^2 - m_i^2 + i0} \cdot \frac{(2k+p)_\nu}{(k+p)^2 - m_i^2 + i0} - (q=p=0) \right). \end{aligned} \quad (\text{B.4})$$

Each integral is made finite by one subtraction at  $q=0$  (first) and  $q=p=0$  (second). This results in one counterterm which renormalizes the charge to its integer value. In the LHZ scheme followed here charge conservation is not protected by logarithmic divergences.

The final expressions in (22) are quoted in terms of

$$\tilde{\mathcal{I}}^i \equiv \epsilon_1 \cdot \epsilon_2 \mathcal{I}^{ii}(q_1 + q_2) + \epsilon_1^\mu \epsilon_2^\nu \mathcal{I}_{\mu\nu}^{ii}(q_1, -q_2). \quad (\text{B.5})$$

Also the contributions from the three-point function in (15) read

$$\begin{aligned} \mathcal{T}_4^{\gamma\gamma\pi^0\pi^0} &= -2i \frac{m_\pi^2}{f_\pi^2} \tilde{\mathcal{I}}^\pi - i \frac{m_K^2}{f_\pi^2} \frac{2\hat{m}}{\hat{m} + m_s} \tilde{\mathcal{I}}^K \\ \mathcal{T}_4^{\gamma\gamma\pi^+\pi^-} &= \mathcal{T}_4^{\gamma\gamma\pi^0\pi^0} \\ \mathcal{T}_4^{\gamma\gamma KK} &= -i \frac{m_\pi^2}{f_K^2} \frac{\hat{m} + m_s}{2\hat{m}} \tilde{\mathcal{I}}^\pi - i \frac{3}{2} \frac{m_K^2}{f_K^2} \tilde{\mathcal{I}}^K \\ \mathcal{T}_4^{\gamma\gamma\eta\eta} &= -i \frac{2}{3} \frac{m_\pi^2}{f_\eta^2} \frac{\hat{m} + 2m_s}{3\hat{m}} \tilde{\mathcal{I}}^\pi - i \frac{5}{3} \frac{m_K^2}{f_\eta^2} \frac{2(\hat{m} + 2m_s)}{3(\hat{m} + m_s)} \tilde{\mathcal{I}}^K \\ \mathcal{T}_4^{\gamma\gamma\pi\eta} &= 0. \end{aligned} \quad (\text{B.6})$$

## B-ii. $\mathbf{VVj_Aj_A}$

The one-loop contribution to the four-point function  $\mathbf{VVj_Aj_A}$  maybe obtained similarly. In particular,

$$\begin{aligned} \langle \mathbf{VVj_Aj_A} \rangle &\equiv \langle 0 | T^* \mathbf{V}_\mu^a(x) \mathbf{V}_\nu^b(y) \mathbf{j}_{A\alpha}^c(z_1) \mathbf{j}_{A\beta}^d(z_2) | 0 \rangle_{\text{con.}} \\ &= -i (f^{iah} f^{hbj} + f^{ibh} f^{haj}) \cdot (f^{jcl} f^{ldi} + f^{jdl} f^{lci}) \delta^4(z_1 - z_2) g_{\alpha\beta} \\ &\quad \times \left( g_{\mu\nu} \delta^4(x - y) \int_q e^{-iq \cdot (y-z)} \mathcal{I}^{ij}(q) + \int_p \int_q e^{iq \cdot x - iq \cdot y - i(q-p) \cdot z} \mathcal{I}_{\mu\nu}^{ij}(q, p) \right). \end{aligned} \quad (\text{B.7})$$

Since we need the integrated version, then

$$\begin{aligned} i \int \langle \mathbf{VVj_Aj_A} \rangle &\equiv i \int_x \int_y e^{iq_1 \cdot x - iq_2 \cdot y} \left\langle 0 \left| \hat{S} T^* \left[ \left( \mathbf{V}^{\mu,3}(x) + \frac{1}{\sqrt{3}} \mathbf{V}^{\mu,8}(x) \right) \right. \right. \right. \\ &\quad \times \left. \left. \left( \mathbf{V}_\nu^3(y) + \frac{1}{\sqrt{3}} \mathbf{V}_\nu^8(y) \right) \mathbf{j}_{A\alpha}^c(z) \mathbf{j}_{A\beta}^d(0) \right] \right| 0 \right\rangle \end{aligned}$$

$$= 2 \times \left\{ \begin{array}{|c|c|c|} \hline (c, d) & \text{SU(3)meson} & \text{contribution} \\ \hline (1, 1), (2, 2) & \pi^\pm & \mathcal{I}^\pi + \frac{1}{2}\mathcal{I}^K \\ (3, 3) & \pi^0 & 2\mathcal{I}^\pi + \frac{1}{2}\mathcal{I}^K \\ (4, 4), (5, 5) & K^\pm & \frac{1}{2}\mathcal{I}^\pi + \mathcal{I}^K \\ (6, 6), (7, 7) & K^{0\bar{0}} & \frac{1}{2}\mathcal{I}^\pi + \frac{1}{2}\mathcal{I}^K \\ (8, 8) & \eta & \frac{3}{2}\mathcal{I}^K \\ (3, 8) & (\pi^0, \eta) & \frac{\sqrt{3}}{2}\mathcal{I}^K \\ \hline \end{array} \right. \quad (\text{B.8})$$

where  $\mathcal{I}^i$  ( $\tilde{\mathcal{I}}^i(q_1, q_2) \equiv \mathcal{I}^i(q_1, -q_2)$ ) is defined as

$$\mathcal{I}^i(q_1, q_2) \equiv g_{\mu\nu} \mathcal{I}^{ii}(q_1 - q_2) + \mathcal{I}_{\mu\nu}^{ii}(q_1, q_2) . \quad (\text{B.9})$$

The respective contributions to (15) from  $\langle \mathbf{V}\mathbf{V}_A \mathbf{j}_A \mathbf{j}_A \rangle$  are

$$\begin{aligned} (\pi^0, \pi^0) &: -i2k_1 \cdot k_2 f_\pi^{-2} (2\tilde{\mathcal{I}}^\pi + \frac{1}{2}\tilde{\mathcal{I}}^K) \\ (\pi^+, \pi^-) &: -i2k_1 \cdot k_2 f_\pi^{-2} (\tilde{\mathcal{I}}^\pi + \frac{1}{2}\tilde{\mathcal{I}}^K) \\ (\mathbf{K}^+, \mathbf{K}^-) &: -i2k_1 \cdot k_2 f_K^{-2} (\frac{1}{2}\tilde{\mathcal{I}}^\pi + \tilde{\mathcal{I}}^K) \\ (K^0, \bar{K}^0) &: -i2k_1 \cdot k_2 f_K^{-2} (\frac{1}{2}\tilde{\mathcal{I}}^\pi + \frac{1}{2}\tilde{\mathcal{I}}^K) \\ (\eta, \eta) &: -i2k_1 \cdot k_2 f_\eta^{-2} (\frac{3}{2}\tilde{\mathcal{I}}^K) \\ (\pi^0, \eta) &: -i2k_1 \cdot k_2 f_\pi^{-1} f_\eta^{-1} (\frac{\sqrt{3}}{2}\tilde{\mathcal{I}}^K) \end{aligned} \quad (\text{B.10})$$

with  $k_1 \cdot k_2 = (s - m_1^2 - m_2^2)/2$ .

## APPENDIX C : $\Sigma$ MODEL

In this Appendix we provide a simple implementation of the resonance saturation analysis at tree level in the context of the linear sigma-model. This complements our general analysis in section V.

### C-i. Lagrangian

Consider the linear sigma-model with general (quadratic) couplings to vector and axial-vectors with global chiral symmetry

$$\begin{aligned} \mathcal{L}_\Sigma &= \frac{1}{4} \text{Tr} [D_\mu \Sigma D^\mu \Sigma^\dagger] \\ \mathcal{L}_{kin} &= \text{Tr} \left( -\frac{1}{4} (F_{l,r}^{\mu\nu})^2 + \frac{m^2}{2} (A_{l,r}^\mu)^2 \right) \\ \mathcal{L}_{int} &= \frac{1}{4} b_1 g^2 \text{Tr} [\Sigma \Sigma^\dagger] \text{Tr} \left( (A_{l,r}^\mu)^2 \right) - b_2 g^2 \text{Tr} [A_l^\mu \Sigma A_r^\mu \Sigma^\dagger] \\ &\quad - b_3 g^2 \text{Tr} [A_l^\mu A_{l,\mu} \Sigma \Sigma^\dagger] - b_4 g^2 \text{Tr} [A_r^\mu A_{r,\mu} \Sigma^\dagger \Sigma] \end{aligned} \quad (\text{C.1})$$

where

$$\begin{aligned} \Sigma &= (\hat{\sigma}^0 - C) \mathbf{1} + \sigma^h \lambda^h + i\pi^a \lambda^a \\ D^\mu \Sigma &= \partial^\mu \Sigma - ig(A_l^\mu \Sigma - \Sigma A_r^\mu) \\ F_{l,r}^{\mu\nu} &= \partial^\mu A_{l,r}^\nu - \partial^\nu A_{l,r}^\mu - ig[A_{l,r}^\mu, A_{l,r}^\nu], \end{aligned} \quad (\text{C.2})$$

where  $-C$  is the vacuum expectation value of  $\sigma^0$ , and the vector field is given as

$$A_{l,r}^\mu = (\vec{v}^\mu \pm \vec{a}^\mu) \cdot \vec{\lambda} . \quad (\text{C.3})$$

The  $vv\sigma$ -vertex comes only from  $\mathcal{L}_{int}$ ,

$$\mathcal{L}_{vv\sigma} = 4(b_1 - b_2 - b_3 - b_4)g^2 C v_\mu^a v^{\mu,a} \hat{\sigma}_0 - 4(b_2 + b_3 + b_4)g^2 C d^{abh} v_\mu^a v^{\mu,b} \sigma^h . \quad (\text{C.4})$$



The  $aa\sigma$ -vertex comes from both  $\mathcal{L}_\Sigma$  and  $\mathcal{L}_{int}$ ,

$$\mathcal{L}_{aa\sigma} = 4(b_1 + b_2 - b_3 - b_4 - 1)g^2 C a_\mu^a a^{\mu,a} \hat{\sigma}_0 + 4(b_2 - b_3 - b_4)g^2 C d^{abh} a_\mu^a a^{\mu,b} \sigma^h. \quad (C.5)$$

One can recombine the couplings so that

$$\begin{aligned} \mathcal{L}_{vv\sigma} &= 4(\tilde{b}_1 + \tilde{b}_2) C v_\mu^a v^{\mu,a} \hat{\sigma}_0 + 4\tilde{b}_2 C d^{abh} v_\mu^a v^{\mu,b} \sigma^h \\ \mathcal{L}_{aa\sigma} &= 4(\tilde{b}_1 + \tilde{b}_3 - 1) C a_\mu^a a^{\mu,a} \hat{\sigma}_0 + 4\tilde{b}_3 C d^{abh} a_\mu^a a^{\mu,b} \sigma^h \end{aligned} \quad (C.6)$$

with the dimensionless couplings,  $\tilde{b}_1 \equiv b_1 g^2$ ,  $\tilde{b}_2 \equiv -(b_2 + b_3 + b_4)g^2$  and  $\tilde{b}_3 \equiv (b_2 - b_3 - b_4)g^2$ . The vector meson vertices  $vvv$  and  $vaa$  stem only from the kinetic part of the vector meson Lagrangian

$$\begin{aligned} \mathcal{L}_{vaa} &= -4g f^{abc} \{v_\nu^a (\partial^\mu a^{\nu,b}) a_\mu^c + (\partial^\mu v_\nu^a) a_\mu^b a^{\nu,c} + v_\mu^a A_\nu^b (\partial^\mu a^{\nu,c})\} \\ \mathcal{L}_{vvv} &= -4g f^{abc} v_\nu^a (\partial^\mu v^{\nu,b}) v_\mu^c. \end{aligned} \quad (C.7)$$

Here the three point vector vertex is fixed by the gauge coupling  $g$  and the structure constants. The vector meson propagator is

$$\Pi_v^{\mu\nu} = \frac{i}{q^2 - m_v^2} \left( g^{\mu\nu} - \frac{q^\mu q^\nu}{m_v^2} \right), \quad (C.8)$$

and similarly for the axial vector particles.

### C-ii. Various Contributions

The tree contribution to  $\mathbf{V}\mathbf{V}\sigma_0$  is

$$\mathcal{T}_{vv\sigma_0}^{ab} = i \frac{8}{3} (\tilde{b}_1 + \tilde{b}_2) \epsilon_1 \cdot \epsilon_2 \delta^{ab} \delta^{cd} \frac{C M_a}{E_a^2} (f_{v_c} f_{v_d} m_{v_c} m_{v_d}) \frac{i}{q_{v_c}^2 - m_{v_c}^2} \frac{i}{s - m_{\sigma_0}^2} \langle 0 | \bar{q} q | \sigma \rangle \frac{i}{q_{v_c}^2 - m_{v_c}^2} \quad (C.9)$$

where  $\langle 0 | \bar{q} q | \sigma \rangle = \lambda_0^2$ . Since the photon is on mass-shell only the combination  $\epsilon_1 \cdot \epsilon_2$  appear after contractions,

$$\epsilon_1^\mu \Pi_v^{c,\mu\gamma} \Pi_v^{d,\gamma\nu} \epsilon_2^\nu = \epsilon_1 \cdot \epsilon_2 \frac{i}{q_1^2 - m_{v_c}^2} \frac{i}{q_2^2 - m_{v_d}^2}. \quad (C.10)$$

The tree contribution to  $\mathbf{V}\mathbf{V}\sigma^h$  is

$$\mathcal{T}_{vv\sigma^h}^{ab} = -i 4 \tilde{b}_2 \epsilon_1 \cdot \epsilon_2 d^{abh} d^{cdh} \frac{C M_b}{E_a E_b} (f_{v_c} f_{v_d} m_{v_c} m_{v_d}) \frac{i}{q_{v_c}^2 - m_{v_c}^2} \frac{i}{s - m_{\sigma_0}^2} \langle 0 | \bar{q} \lambda^h q | \sigma^h \rangle \frac{i}{q_{v_c}^2 - m_{v_c}^2}, \quad (C.11)$$

where  $\langle 0 | \bar{q} \lambda^h q | \sigma^h \rangle = \lambda_h^2$ .

The  $\sigma_0$  contribution to  $\mathbf{V}\mathbf{V}\mathbf{j}_A \mathbf{j}_A$  is

$$\begin{aligned} \mathcal{T}_{vvaa}^{ab} &= \delta^{cd} \delta^{ab} \epsilon_1 \cdot \epsilon_2 \frac{1}{E_a E_b} \frac{i f_{v_c} m_{v_c}}{q_{v_c}^2 - m_{v_c}^2} \frac{i f_{v_d} m_{v_d}}{q_{v_d}^2 - m_{v_d}^2} \left( 16(\tilde{b}_1 + \tilde{b}_2)(\tilde{b}_1 + \tilde{b}_3 - 1) C^2 \right) \frac{i}{s - m_{\sigma_0}^2} \\ &\quad \times (f_{a_a} m_{a_a} f_{a_b} m_{a_b}) \times k_a^\alpha \Pi_a^{a,\alpha\gamma} \Pi_a^{a,\gamma\beta} k_b^\beta, \end{aligned} \quad (C.12)$$

with

$$k_1^\alpha \Pi_a^{a,\alpha\gamma} \Pi_a^{b,\gamma\beta} k_2^\beta = k_1 \cdot k_2 \left( 1 - \frac{k_1^2}{m_{a_a}^2} - \frac{k_2^2}{m_{a_b}^2} + \frac{k_1^2}{m_{a_a}^2} \frac{k_2^2}{m_{a_b}^2} \right) \frac{i}{k_1^2 - m_{a_a}^2} \frac{i}{k_2^2 - m_{a_b}^2}. \quad (C.13)$$

The  $\sigma_h$  contribution to  $\mathbf{V}\mathbf{V}\mathbf{j}_A \mathbf{j}_A$  is

$$\begin{aligned} \mathcal{T}_{vvaa}^{ab} &= d^{cdh} d^{abh} \epsilon_1 \cdot \epsilon_2 \frac{1}{E_a E_b} \frac{i f_{v_c} m_{v_c}}{q_{v_c}^2 - m_{v_c}^2} \frac{i f_{v_d} m_{v_d}}{q_{v_d}^2 - m_{v_d}^2} \left( 16 \tilde{b}_2 \tilde{b}_3 C^2 \right) \frac{i}{s - m_{\sigma_h}^2} \\ &\quad \times (f_{a_a} m_{a_a} f_{a_b} m_{a_b}) k_a^\alpha \Pi_a^{a,\alpha\gamma} \Pi_a^{b,\gamma\beta} k_b^\beta. \end{aligned} \quad (C.14)$$

In Fig. 1-(b), the contribution from the intermediate  $\mathbf{V}$  vanishes because of the SU(3) structure constant  $f^{abc}$ . The contribution from Fig. 1-(c) results in

$$\begin{aligned} \mathcal{T}_{vva a}^{ab} = & i^2 f^{caf} f^{dbf} \frac{1}{E_a E_b} \left( \frac{i f_{v_c} m_{v_c}}{q_1^2 - m_{v_c}^2} \right) \left( \frac{i f_{v_d} m_{v_d}}{q_2^2 - m_{v_d}^2} \right) \left( \frac{i}{t - m_{a_f}^2} \right) \left( \frac{i f_{v_a} m_{a_a}}{k_1^2 - m_{a_a}^2} \right) \left( \frac{i f_{v_b} m_{a_b}}{k_2^2 - m_{a_b}^2} \right) \\ & (-4g)^2 \left[ (\epsilon_1 \cdot k_1)(\epsilon_2 \cdot k_2) \left( 1 - \frac{(k_1 - q_1)^2}{m_{a_f}^2} \right) \left( (k_1 - q_1)(k_2 - q_2) + k_1^2 + k_2^2 - \frac{(k_1 \cdot q_1)^2}{m_{a_a}^2} - \frac{(k_2 \cdot q_2)^2}{m_{a_b}^2} \right) \right. \\ & \left. + \left( \epsilon_1 \cdot \epsilon_2 + \frac{(\epsilon_1 \cdot k_1)(\epsilon_2 \cdot k_2)}{m_{a_f}^2} \right) \left( k_1^2 - \frac{(k_1 \cdot q_1)^2}{m_{a_a}^2} \right) \left( k_2^2 - \frac{(k_2 \cdot q_2)^2}{m_{a_b}^2} \right) \right]. \end{aligned} \quad (\text{C.15})$$

One can generally redefine the couplings,

$$\begin{aligned} \tilde{c}_0 f_\pi &\equiv \frac{2}{3}(\tilde{b}_1 + \tilde{b}_2) C \lambda_0^2 \\ \tilde{c}_{h=3,8} f_\pi &\equiv -\tilde{b}_2 C \lambda_{h=3,8}^2 \\ \tilde{g}_1 f_\pi^2 &\equiv (\tilde{b}_1 + \tilde{b}_2)(\tilde{b}_1 + \tilde{b}_3 - 1) C^2 \\ \tilde{g}_2 f_\pi^2 &\equiv \tilde{b}_2 \tilde{b}_3 C^2 \\ \tilde{g}_3 &\equiv (-g^2) \end{aligned} \quad (\text{C.16})$$

giving in total six independent parameters.

### C-iii. Final Result

$\sigma_0$  and  $\sigma_h$  contributions to  $\mathbf{V}\mathbf{V}\sigma$  :

$$\begin{aligned} \mathcal{T}_{vv\sigma_0}^{ab} &= 4\tilde{c}_0 f_\pi \epsilon_1 \cdot \epsilon_2 \delta^{ab} \delta^{cd} \frac{M_a}{E_a^2} \frac{f_{v_c} f_{v_d}}{m_{v_c} m_{v_d}} \frac{1}{s - m_{\sigma_0}^2} \\ \mathcal{T}_{vv\sigma_h}^{ab} &= 4\tilde{c}_h f_\pi \epsilon_1 \cdot \epsilon_2 d^{abh} d^{cdh} \frac{M_b}{E_a E_b} \frac{f_{v_c} f_{v_d}}{m_{v_c} m_{v_d}} \frac{1}{s - m_{\sigma_0}^2}, \end{aligned} \quad (\text{C.17})$$

where the couplings  $c_{0,8}$  will be fixed empirically.

$\sigma_0$  contribution to  $\mathbf{V}\mathbf{V}\mathbf{j}_A\mathbf{j}_A$  :

$$\begin{aligned} \mathcal{T}_{vva a}^{ab} &= i16\tilde{g}_1 f_\pi^2 \delta^{cd} \delta^{ab} \epsilon_1 \cdot \epsilon_2 \frac{1}{E_a E_b} \frac{f_{v_c} f_{v_d}}{m_{v_c} m_{v_d}} \frac{1}{s - m_{\sigma_0}^2} \\ &\times k_1 \cdot k_2 \left( 1 - \frac{m_a^2}{m_{a_a}^2} - \frac{m_b^2}{m_{a_b}^2} + \frac{m_a^2}{m_{a_a}^2} \frac{m_b^2}{m_{a_b}^2} \right) \frac{f_{a_a} m_{a_a}}{m_a^2 - m_{a_a}^2} \frac{f_{a_b} m_{a_b}}{m_b^2 - m_{a_b}^2}. \end{aligned} \quad (\text{C.18})$$

$\sigma_h$  contribution to  $\mathbf{V}\mathbf{V}\mathbf{j}_A\mathbf{j}_A$  :

$$\begin{aligned} \mathcal{T}_{vva a}^{ab} &= i16\tilde{g}_2 f_\pi^2 d^{cdh} d^{abh} \epsilon_1 \cdot \epsilon_2 \frac{1}{E_a E_b} \frac{f_{v_c} f_{v_d}}{m_{v_c} m_{v_d}} \frac{1}{s - m_{\sigma_h}^2} \\ &\times k_1 \cdot k_2 \left( 1 - \frac{m_a^2}{m_{a_a}^2} - \frac{m_b^2}{m_{a_b}^2} + \frac{m_a^2}{m_{a_a}^2} \frac{m_b^2}{m_{a_b}^2} \right) \frac{f_{a_a} m_{a_a}}{m_a^2 - m_{a_a}^2} \frac{f_{a_b} m_{a_b}}{m_b^2 - m_{a_b}^2}. \end{aligned} \quad (\text{C.19})$$

Axial-vector contributions to  $\mathbf{V}\mathbf{V}\mathbf{j}_A\mathbf{j}_A$  :

$$\begin{aligned} \mathcal{T}_{vva a}^{ab} &= -i16g_3 f^{caf} f^{dbf} \frac{1}{E_a E_b} \left( \frac{f_{v_c} f_{v_d}}{m_{v_c} m_{v_d}} \right) \left( \frac{1}{t - m_{a_f}^2} \right) \left( \frac{f_{v_a} m_{a_a}}{m_a^2 - m_{a_a}^2} \right) \left( \frac{f_{v_b} m_{a_b}}{m_b^2 - m_{a_b}^2} \right) \\ &\left[ (\epsilon_1 \cdot k_1)(\epsilon_2 \cdot k_2) \left( 1 - \frac{t}{m_{a_f}^2} \right) \left( -t + m_a^2 + m_b^2 - \frac{(k_1 \cdot q_1)^2}{m_{a_a}^2} - \frac{(k_2 \cdot q_2)^2}{m_{a_b}^2} \right) \right. \\ &\left. + \left( \epsilon_1 \cdot \epsilon_2 + \frac{(\epsilon_1 \cdot k_1)(\epsilon_2 \cdot k_2)}{m_{a_f}^2} \right) \left( m_a^2 - \frac{(k_1 \cdot q_1)^2}{m_{a_a}^2} \right) \left( m_b^2 - \frac{(k_2 \cdot q_2)^2}{m_{a_b}^2} \right) \right] \\ &+ (t, a, k_1 \leftrightarrow u, b, k_2). \end{aligned} \quad (\text{C.20})$$

In the text, these couplings are redefined in terms of dimensionless couplings.